ORIGINAL ARTICLE doi: 10.2176/nmc.oa.2018-0287

Neurol Med Chir (Tokyo) 59, 176–183, 2019 Online April 17, 2019

Usefulness of [11C] Methionine PET in the Differentiation of Tumefactive Multiple Sclerosis from High Grade Astrocytoma

Satoka HASHIMOTO,[1] Motoki INAJI,[1,2] Tadashi NARIAI,[1,2] Daisuke KOBAYASHI,[3] Nobuo SANJO,[4] Takanori YOKOTA,[4] Kenji ISHII,[2] and Maehara TAKETOSHI[1]

[1]Department of Neurosurgery, Tokyo Medical and Dental University, Tokyo, Japan;
[2]Research Team for Neuroimaging, Tokyo Metropolitan Institute of Gerontology, Tokyo, Japan;
[3]Department of Human Pathology, Tokyo Medical and Dental University, Tokyo, Japan;
[4]Department of Neurology and Neurological Science, Tokyo Medical and Dental University, Tokyo, Japan

Abstract

Tumefactive multiple sclerosis (tumefactive MS) is an atypical variant of MS characterized by a large isolated demyelinating lesion. Because tumefactive MS mimics high grade astrocytoma clinically and radiologically, it is difficult to distinguish between the two using only traditional diagnostic modalities, such as routine magnetic resonance imaging. [11C] methionine positron emission tomography (MET PET) has been known as a useful diagnostic tool for glioma. However, it has not been established as a diagnostic tool for tumefactive MS yet. Therefore, the objective of this study was to evaluate the performance of MET PET in differentiating tumefactive MS from high grade astrocytoma. We studied patients with tumefactive MS [six patients (three men, three women), 7 lesions] and 77 patients with astrocytoma (World Health Organization grade II: 13 patients, grade III: 28 patients, and grade IV: 36 patients), and we compared MET uptake of tumefactive demyelinating lesions and astrocytoma. For MET PET analysis, Lesion/Normal region ratios (L/N ratios) were calculated and compared between tumefactive demyelinating lesions and astrocytoma. On MET PET, the L mean/N ratio of tumefactive MS was 1.18 ± 0.50, which was significantly lower than that of high-grade glioma (astrocytoma grade III: 1.95 ± 0.62, *P* = 0.006; grade IV: 2.35 ± 0.54, *P* <0.0001). The L maximum (L max)/N ratio of tumefactive demyelinating lesion was also significantly lower than that of high grade astrocytoma (tumefactive MS: 1.89 ± 0.55; astrocytoma grade III: 3.37 ± 1.36, *P* = 0.0232; astrocytoma grade IV: 4.35 ± 1.30, *P* <0.0001). In conclusion, MET PET can help differentiate tumefactive MS from high grade astrocytoma.

Key words: tumefactive multiple sclerosis, methionine PET, high grade astrocytoma

Introduction

Multiple sclerosis (MS) is the most common inflammatory demyelinating disease of the central nervous system defined by multiple separate attacks on the brain and spinal cord.[1)] Tumefactive MS is a rare variant of MS characterized by an acute, large tumor-like demyelinating lesion.[2–4)]

It is a challenge to differentiate tumefactive MS from brain tumors, especially high grade astrocytoma because tumefactive MS mimics brain tumors clinically and radiologically.[5,6)] Patients with tumefactive MS are often polysymptomatic because of the large size of the lesion[3)]; additionally, the neurological symptoms induced by tumefactive MS are often observed for the first time (53–78%).[2,3,7)] Moreover, the clinical course of tumefactive MS is usually rapidly progressive.[8)] On magnetic resonance imaging (MRI), tumefactive MS appears as an isolated demyelinating lesion measuring over 2 cm with mass effect, perifocal edema, a T_2-hypointense rim, and ring enhancement with gadolinium (Gd).[2)]

Many studies have reported the usefulness of [11C] methionine positron emission tomography (MET PET) for diagnosing and grading glioma,[9–13)] and the surgical strategies combining MET PET were also indicated to improve the surgical outcome of glioma.[14)]

Received November 21, 2018; Accepted January 22, 2019

However, few previous studies have reported about the MET uptake of tumefactive demyelinating lesions. The usefulness of MET PET in patients with tumefactive MS is still unclear. Therefore, our objective was to clarify the usefulness of MET PET for diagnosing tumefactive MS.

Patients and Methods

Patients

We studied patients with tumefactive MS and patients with newly-diagnosed astrocytoma in the Tokyo Medical and Dental University Hospital from 2006 to date. Six patients with 7 tumefactive demyelinating lesions in the brain were included in this study (three men, three women; mean age, 48.7 ± 14.1 years; age range, 32–74 years). All patients presented with sudden neurological deficits and progressive clinical courses; therefore, they were suspected to have a malignant brain tumor. The diagnosis of tumefactive MS was confirmed either pathologically (3 lesions in two men and one woman) or clinically (4 lesions in two men and two women) based on clinical follow-up with neurologic findings, imaging findings, and results of cerebrospinal fluid (CSF) analysis. For immunohistochemical staining of inflammatory cells, we used anti-CD3 antibody (Leica, LN10), anti-CD20 antibody (Agilent, L-26), and anti-CD68 antibody (Agilent, KP-1). Seventy-seven patients with newly-diagnosed astrocytoma were compared with patients with tumefactive MS to clarify the difference of MET uptake [36 men, 31 women; mean age, 53.3 ± 17.5 years; age range, 16–79 years, World Health Organization (WHO) grade II: 13 patients (mean age ± standard deviation {SD} = 53.3 ± 19.6), grade III: 28 patients (mean age ± SD = 46.4 ± 17.2), grade IV: 36 patients (mean age ± SD = 58.8 ± 15.4)]. Astrocytoma was diagnosed by pathological results according to the Central Nervous System WHO 2007 Classification. This study was approved by the Ethics Committees of Tokyo Medical and Dental University. Informed consent was obtained from the patients.

Clinical courses of tumefactive MS

Patients' clinical histories were investigated retrospectively. To visualize patients' general condition, their Karnofsky Performance Status (KPS) was scored before the onset of symptoms and on admission. Additionally, the duration from the onset to hospitalization was calculated to determine whether their clinical course was progressive.

Diagnostic examinations for tumefactive MS

We reviewed the data from MRI and CSF examinations [cell counts, total protein level, myelin basic protein (MBP), oligoclonal bands (OCBs), and immunoglobulin G (IgG) index], anti-Aquaporin4 (AQP4) antibody in the serum, and MET PET scans. CSF and serum samples of all patients were taken concurrently. We assessed the levels of albumin (Alb) and IgG in the serum and CSF, and OCBs, and calculated the IgG index as follows: (CSF – IgG/CSF – Alb)/(serum – IgG/serum – Alb).

[^{11}C] methionine positron emission tomography

Positron emission tomography measurements were determined using a PET scanner (Headtome IV or V, Shimadzu, Kyoto) and measuring the equilibrated radioactivity 20 min after an intravenous injection of MET (250–350 MBq). The transmission data were acquired for each patient with a rotating germanium-68 rod source for attenuation correction. The regional uptake of MET PET was expressed as the standardized uptake volume (SUV) [(tissue activity {Bq}/tissue volume {ml})/(injected radioisotope activity {Bq}/body weight {g})], and the tracer uptake by the tumefactive demyelinating lesion or astrocytoma was expressed as the ratio of SUV mean or SUV max of the lesion to that of the normal contralateral frontal lobe (lesion/normal region ratio: L mean/N ratio [SUV mean of the lesion/SUV mean of the normal region]) and L max/N ratio (SUV max of the lesion/SUV mean of the normal region), respectively. To determine the SUV of the lesion, we placed regions of interest manually around the lesion.

Statistical analysis

The L mean/N ratio and L max/N ratio are presented as a mean ± SD. Statistical analyses for group comparisons were performed by analysis of variance followed by Tukey's post-hoc test using GraphPad Prism version 6.05 (GraphPad Software, La Jolla, CA, USA). A difference between groups was considered significant when the *P*-value was <0.05.

Results

The clinical characteristics of patients with tumefactive MS are displayed in Table 1. Three of six patients were diagnosed as having tumefactive MS based on pathological findings, and the other three patients were diagnosed based on their aggressive clinical courses and good response to treatment. All six patients developed various neurological deficits rapidly. In five of six cases, the KPS score deteriorated to about 50 from 100 between 1 and 2 months. We could not differentiate tumefactive MS from high grade astrocytoma by patients' clinical courses. Five patients were treated by corticosteroid therapy, and one patient was treated by corticosteroid

Table 1 Clinical data

Patient no.	Tumefactive demyelinating lesion no.	MET PET		The period from the onset to hospitalization (days)	KPS	MRI			FDG PET SUV max	CSF examination					Anti-AQP4 antibody	Biopsy	Treatment
		T mean/N ratio	T max/N ratio		Before the onset	On admission	Gd ring enhancement	Perifocal edema		WBC (cells/ml)	Total protein (mg/dl)	MBP (pg/ml)	OCBs	IgG index			
1	Lesion 1	1.28	1.9	35	100	60	(+)	(+)	4.3	2	38	451	(–)	(–)	(–)	No	Corticosteroid and plasma exchange
2 Representative case 1	Lesion 2	1.77	2.63	20	100	40	(+)	(+)	5.6	4	32	<31.3	(–)	(–)	N.A.	Yes	Corticosteroid
3	Lesion 3	1.29	2.05	60	100	90	(+)	(+)	5.7	4	48	N.A.	(–)	(–)	N.A.	No	Corticosteroid
4	Lesion 4	1.6	2.44	30	100	60	(+)	(+)	N.A.	7	46	1300	N.A.	(–)	N.A.	Yes	Corticosteroid
5 Representative case 2	Lesion 5	1.29	1.7	60	100	40	(–)	(–)	5.7	40	85	509	(–)	(–)	(–)	No Yes	Corticosteroid
	Lesion 6	0.326	1.36				(–)	(+)	2.7								
6	Lesion 7	0.72	1.12	30	100	40	(+)	(+)	N.A.	49	58	<31.3	(–)	(–)	N.A.	No	Corticosteroid

Anti-AQP4 antibody: anti-aquaporin 4 antibody, FDG PET: ^{18}F-fluorodeoxyglucose positron emission tomography, Gd: gadolinium, IgG: immunoglobulin G, KPS: Karnofsky performance status, MET PET: [^{11}C] methionine positron emission tomography, MBP: myelin basic protein, MRI: magnetic resonance imaging, OCBs: oligoclonal bands, T mean/N ratio: mean standardized uptake volume of tumefactive multiple sclerosis tissue to that of normal tissue, T max/N ratio: maximum standardized uptake volume of tumefactive multiple sclerosis tissue to that of normal tissue, WBC: white blood cell.

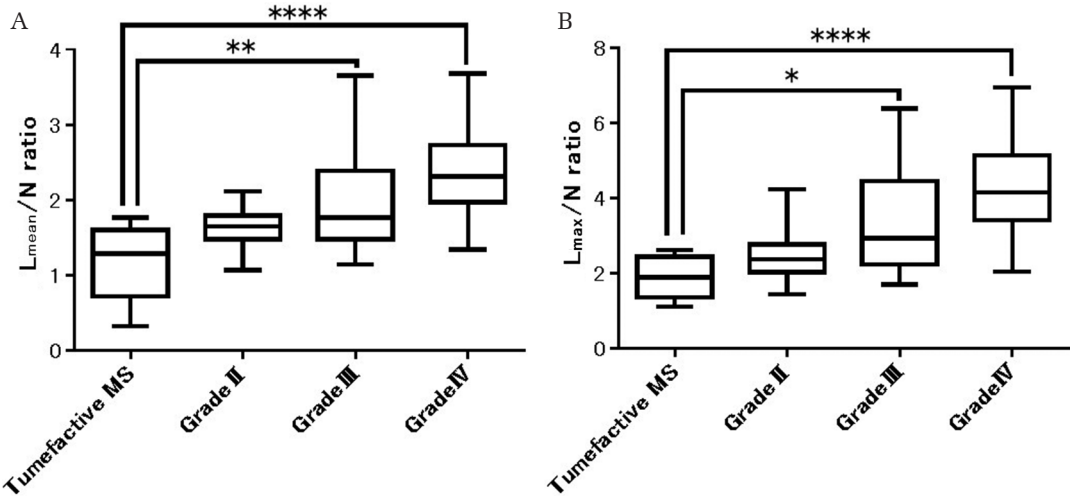

Fig. 1 Box plots comparing the L mean/N ratio (A) and L max ratio (B) of astrocytoma and tumefactive demyelinating lesions. Horizontal bars inside the boxes indicate median values. The top of the error bar indicates the maximum, whereas the bottom indicates the minimum value. MS, multiple sclerosis. $^{*}P$ <0.05, $^{**}P$ <0.01, $^{***}P$ <0.001, $^{****}P$ <0.0001.

therapy and plasma exchange. In all patients, the neurological deficits improved rapidly after treatment, and all the lesions decreased in size and some lesions were diminished by these therapies.

Magnetic resonance imaging demonstrated Gd ring enhancement in 5 of 7 lesions and perifocal edema in 6 lesions. Most lesions showed both Gd enhancement and perifocal edema that mimicked high grade astrocytoma (representative case 1). One lesion without Gd enhancement had perifocal edema; therefore, high grade astrocytoma was cited as a differential diagnosis (representative case 2). According to the CSF examination, an abnormally increased cell count and total protein level were detected in three of six cases, respectively. In three of six cases, increased MBP was observed. OCBs or an increased IgG index was not found. Anti-AQP4 antibodies were also not detected.

On MET PET, the L mean/N ratio was 1.18 ± 0.50, and L max/N ratio of tumefactive lesions was 1.89 ± 0.55. The L mean/N ratio was significantly lower than that of WHO grade III astrocytoma (P = 0.006) and that of WHO grade IV (P <0.0001) respectively (astrocytoma grade II: 1.63 ± 0.27, grade III: 1.95 ± 0.62, and grade IV: 2.35 ± 0.54) (Fig. 1A). The L max/N ratio was also significantly lower than that of WHO grade III astrocytoma (P = 0.0232) and that of WHO grade IV (P <0.0001) (astrocytoma grade II: 2.50 ± 0.71, grade III: 3.37 ± 1.36, and grade IV: 4.35 ± 1.30) (Fig. 1B). There was a variation of MET uptake depending on the lesion. MET uptake of 5 lesions was relatively high (average L mean/N ratio = 1.44 and average L max/N ratio = 2.14), and the MET uptake of the other 2 lesions was low (average L mean/N ratio = 0.524 and average L max/N ratio = 1.24). In two MET high uptake lesions (lesions 2 and 4), the pathological examination showed that diffuse infiltration of T cells was shown relatively more in the tumefactive demyelinating lesion with high MET uptake than in the lesion with low MET uptake (Figs. 2G–2J). There was little difference of B cells accumulation between MET high uptake lesions and MET low uptake lesion (Figs. 2K and 2L).

Representative case 1

A 74-year-old woman had been treated for rheumatoid arthritis with adalimumab before she developed sudden left facial paralysis with left hemiplegia just 4 days later. The KPS score deteriorated from 100 to 40 over 20 days. MRI demonstrated an isolated lesion (7 × 5 cm) in the subcortex of the right frontotemporal lobe (lesion 1) (Fig. 3). The lesion was hyperintense with perifocal edema on fluid-attenuated inversion recovery (FLAIR) imaging (Fig. 3A). T_1-weighted Gd-enhanced imaging also showed a ring-enhanced lesion (Fig. 3B). According to the CSF examination, the cell count, total protein level, and MBP uptake were normal. OCBs were negative, and the IgG index in the CSF was not increased. MET PET showed a high T/N ratio for the tumefactive lesion (L mean/N ratio = 1.77 and L max/N ratio = 2.63) (Fig. 3C). A biopsy revealed loss of myelin and relative preservation of axons (Figs. 2A and 2C). The infiltration of foamy macrophages without tumor cells was seen (Fig. 2E). The lesion was diagnosed as tumefactive MS. The strong infiltration of T cells was seen diffusely (Fig. 2I). The patient was treated with steroids. The neurological symptoms improved quickly, and the tumefactive lesion was markedly decreased on the MRI scan after treatment.

Representative case 2

A 60-year-old man developed sensory loss in the left lower extremity and then a right visual field

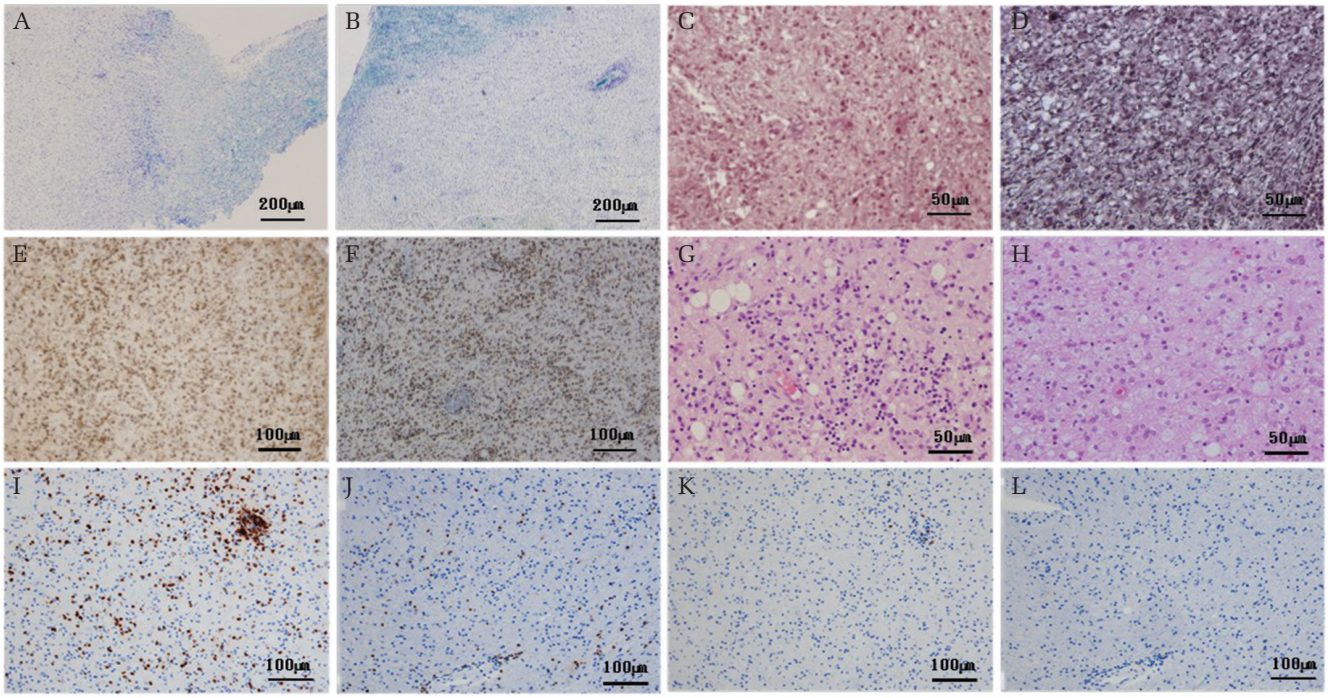

Fig. 2 The pathohistological results of the representative cases. A, C, E, G, I, K: representative case 1; B, D, F, H, J, L: representative case 2. (A and B) Kluver–Barrera staining showing loss of myelin. (C and D) Bodian staining. The axons are relatively preserved. (E and F) Immunohistochemistry for CD68 shows macrophage accumulation. (G and H) Hematoxylin and eosin staining. Infiltration of macrophages and lymphocytes is observed. Tumor cells are not seen. (I and J) Immunohistochemistry for CD3 shows T cells with diffusive accumulation. (K and L) Immunohistochemistry for CD20 shows accumulation of B cells.

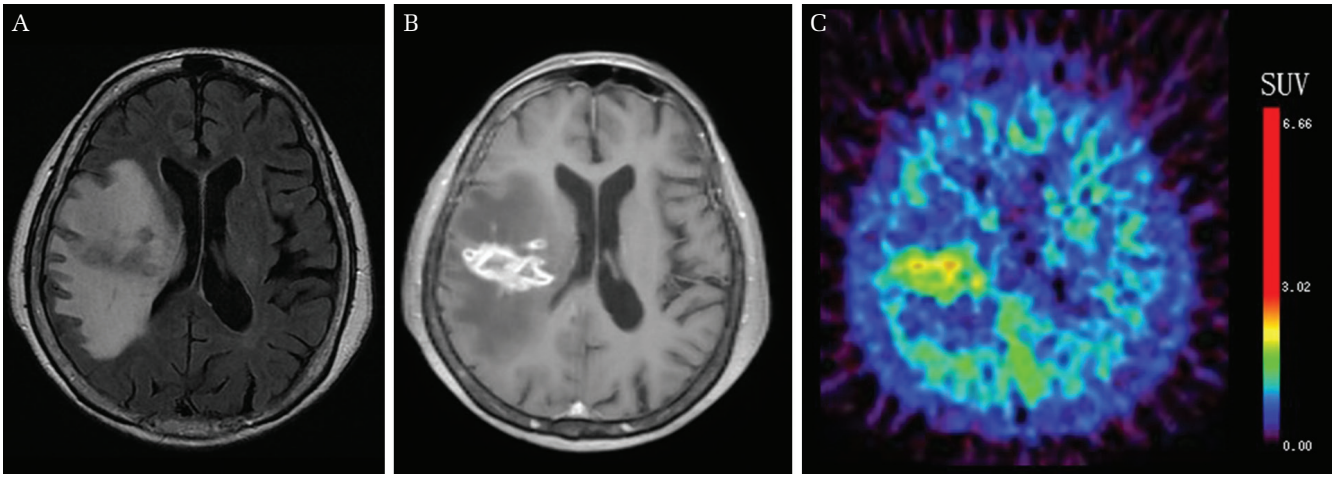

Fig. 3 Preoperative imaging results of representative case 1. (A) Fluid-attenuated inversion recovery image showing perifocal edema. (B) Gadolinium-enhanced magnetic resonance image showing a ring-enhanced lesion in the subcortex of the right frontotemporal lobe. (C) [^{11}C] methionine (MET) positron emission tomography imaging. The tumefactive lesion shows high uptake of [^{11}C] MET (L mean/N ratio = 1.77 and L max/N ratio = 2.63).

defect about 1 month later. The KPS score decreased from 100 to 40 over 60 days. MRI demonstrated 2 tumor-like lesions. One lesion was located in the subcortex of the right occipital lobe (lesion 5), and the other lesion was located in the right side of the pons (lesion 6) (Fig. 4). The occipital lesion was hyperintense on the FLAIR image (Fig. 4A). Although T_1-weighted Gd-enhanced images did not show any Gd enhancement (Fig. 4B), the occipital lesion had perifocal edema (Fig. 4A).

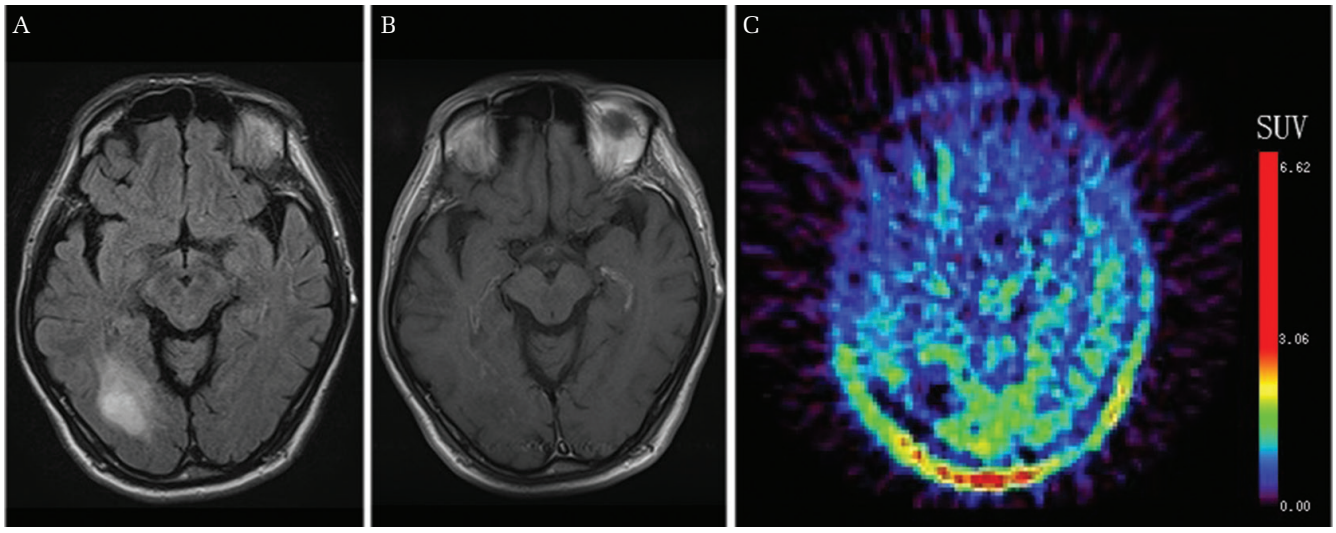

Fig. 4 Preoperative imaging results of representative case 2. (A) Fluid-attenuated inversion recovery image showing a mass lesion and perifocal edema in the subcortex of the left occipital lobe. (B) Gadolinium-enhanced magnetic resonance imaging scan without any enhanced lesions. (C) [^{11}C] methionine (MET) positron emission tomography scan. The tumefactive lesion shows low uptake of [^{11}C] MET (L mean/N ratio = 0.326 and L max/N ratio = 1.36).

Therefore, high grade astrocytoma was suspected as a differential diagnosis in addition to a progressive clinical course. According to the CSF examination, the cell count, total protein level, and MBP uptake were abnormally increased. OCBs or an increased IgG index was not detected. The patient was negative for the anti-AQP4 antibody. On MET PET, the occipital lesion showed low uptake of MET (L mean/N ratio = 0.326 and L max/N ratio = 1.36) (Fig. 4C). A biopsy revealed the loss of myelin, relative preservation of axons and infiltration of foamy macrophages without tumor cells (Figs. 2B, 2D, and 2F). Hence, the diagnosis was tumefactive MS. The infiltration of T cells in this case was less than that in representative case 1 (Figs. 2I and 2J). The patient was treated with a steroid, and then the neurological symptoms improved. Both tumefactive lesions on the MRI scan decreased after treatment.

Discussion

This study demonstrated the usefulness of MET PET for making the differential diagnosis of tumefactive MS from high grade astrocytoma (L mean/N ratio: tumefactive MS 1.18 ± 0.50, astrocytoma grade III: 1.95 ± 0.62 [P = 0.006], grade IV: 2.35 ± 0.54 [P <0.0001]; L max/N ratio: tumefactive MS 1.89 ± 0.55, astrocytoma grade III: 3.37 ± 1.36 [P = 0.0232], grade IV: 4.35 ± 1.30 [P <0.0001]). Both L mean/N ratio and L max/N ratio were useful. Patients with tumefactive MS had rapidly progressive clinical courses and tumor-like lesions on MRI, and it was difficult to diagnose tumefactive MS by only their history and MRI findings. Tumefactive MS can be treated by steroid therapy and/or plasma exchange; therefore, an early and accurate diagnosis is important. The uptake of MET in tumefactive lesions was significantly lower than that in high-grade astrocytoma in our results; thus, MET PET was revealed to be an effective diagnostic tool for discriminating tumefactive MS from high grade astrocytoma.

It is difficult to diagnose tumefactive MS by only classic modalities such as routine MRI or CSF examination. MRI is the most sensitive method for detecting white matter lesions of MS.[2] However, the previous study reported that MRI alone could not provide sufficient information for distinguishing tumefactive demyelinating lesions from gliomas with high accuracy.[15] In addition, Luccuhinetti et al.[2] reported that characteristic MRI features for tumefactive MS were seen in only a limited number of cases. They also showed that a mass effect was observed only in 36% of patients with tumefactive demyelinating diseases, perifocal edema in 77%, ring enhancement in 60–65%, and T_2-hypointense rim in 45%. Our results showed that Gd ring enhancement was positive in 71.4% (5/7 patients) of the lesions, and perifocal edema was positive in 85.7% (6/7). These results were consistent with those of previous reports. A CSF examination is often used for diagnosing MS. Approximately 90% of the patients with MS had unmatched OCBs in the CSF; however, only 52% of patients with tumefactive MS had positive OCBs at their first clinical event.[7] The IgG index was positive in only about 40% of the cases with clinically/radiologically isolated syndrome.[16] In our

study, OCBs and an increased IgG index were not found in the CSF of all patients.

The usefulness of MET PET for diagnosing brain tumors is well established. MET PET has high sensitivity and specificity for detecting high grade astrocytoma.[17] Additionally, many reports concluded that MET PET could discriminate high grade astrocytoma from low grade astrocytoma.[9–13]

A few reports about MET PET showed that MET uptake in tumefactive demyelinating lesions was relatively low.[7,8,18–21] Several case studies demonstrated that the uptake of MET in tumefactive demyelinating lesion was about 1.2–1.5[18,20] (mainly described as the L max/N ratio). Our results were consistent with the findings of these previous studies.

There was variation in the uptake of MET of tumefactive demyelinating lesions in our study. Additionally, the pathological examinations revealed the stronger inflammatory cell infiltration, especially with T cells in lesions with high MET uptake than in those with low MET uptake. The severity of inflammation was supposed to be one of the reasons for variation of MET uptake. MET PET is an imaging method for visualizing amino acid metabolism. A couple of the factors reflecting the MET uptake are increased methionine metabolism and active methionine transport.[22] MET uptake is induced by cell proliferation such as a malignant tumor or the infiltration of cells including inflammation. The other factors are passive diffusion by blood–brain barrier disruption and stagnation of MET in the vascular bed.[18,23] Increased MET uptake was reported in brain abscesses, encephalitis such as Rasmussen syndrome, and anti-*N*-methyl-D-aspartate receptor encephalitis, and radiation necrosis.[22–25] The previous studies reported that increased MET uptake in brain abscesses and encephalitis normalized after treatment, and they concluded that inflammatory cell infiltration was an important factor for MET uptake. Therefore, the severity of inflammation could have effect on MET uptake. However, more histological studies are needed to elucidate the relationship between the severity of inflammation and MET uptake.

In conclusion, MET PET is a promising modality to help make a differential diagnosis between tumefactive MS and high grade astrocytoma because of the significant difference of MET uptake between these two diseases.

Acknowledgments

We thank Dr. Kaoru Tamura, Department of Neurosurgery, Tokyo Medical and Dental University, and Dr. Shihori Hayashi, Department of Neurosurgery, Tokyo Medical and Dental University, for their help in collecting and analyzing data.

Conflicts of Interest Disclosure

All authors have no conflict of interest (COI). Authors who are members of The Japan Neurosurgical Society have registered the self-reported COI disclosure statement form through the website.

References

1) Polman CH, Reingold SC, Banwell B, et al.: Diagnostic criteria for multiple sclerosis: 2010 revisions to the McDonald criteria. *Ann Neurol* 69: 292–302, 2011
2) Lucchinetti CF, Gavrilova RH, Metz I, et al.: Clinical and radiographic spectrum of pathologically confirmed tumefactive multiple sclerosis. *Brain* 131: 1759–1775, 2008
3) Frederick MC, Cameron MH: Tumefactive demyelinating lesions in multiple sclerosis and associated disorders. *Curr Neurol Neurosci Rep* 16: 26, 2016
4) Algahtani H, Shirah B, Alassiri A: Tumefactive demyelinating lesions: a comprehensive review. *Mult Scler Relat Disord* 14: 72–79, 2017
5) Hardy TA, Chataway J: Tumefactive demyelination: an approach to diagnosis and management. *J Neurol Neurosurg Psychiatr* 84: 1047–1053, 2013
6) Tarkkonen A, Rissanen E, Tuokkola T, Airas L: Utilization of PET imaging in differential diagnostics between a tumefactive multiple sclerosis lesion and low-grade glioma. *Mult Scler Relat Disord* 9: 147–149, 2016
7) Altintas A, Petek B, Isik N, et al.: Clinical and radiological characteristics of tumefactive demyelinating lesions: follow-up study. *Mult Scler* 18: 1448–1453, 2012
8) Ninomiya S, Hara M, Morita A, et al.: Tumefactive demyelinating lesion differentiated from a brain tumor using a combination of magnetic resonance imaging and (11)C-methionine positron emission tomography. *Intern Med* 54: 1411–1414, 2015
9) Nariai T, Tanaka Y, Wakimoto H, et al.: Usefulness of L-[methyl-^{11}C] methionine-positron emission tomography as a biological monitoring tool in the treatment of glioma. *J Neurosurg* 103: 498–507, 2005
10) Singhal T, Narayanan TK, Jacobs MP, Bal C, Mantil JC: ^{11}C-methionine PET for grading and prognostication in gliomas: a comparison study with ^{18}F-FDG PET and contrast enhancement on MRI. *J Nucl Med* 53: 1709–1715, 2012
11) Kato T, Shinoda J, Nakayama N, et al.: Metabolic assessment of gliomas using ^{11}C-methionine, [^{18}F] fluorodeoxyglucose, and ^{11}C-choline positron-emission tomography. *AJNR Am J Neuroradiol* 29: 1176–1182, 2008
12) Falk Delgado A, Falk Delgado A: Discrimination between primary low-grade and high-grade glioma with (11)C-methionine PET: a bivariate diagnostic test

accuracy meta-analysis. *Br J Radiol* 91: 20170426, 2018
13) Shinozaki N, Uchino Y, Yoshikawa K, et al.: Discrimination between low-grade oligodendrogliomas and diffuse astrocytoma with the aid of ^{11}C-methionine positron emission tomography. *J Neurosurg* 114: 1640–1647, 2011
14) Ideguchi M, Nishizaki T, Ikeda N, et al.: A surgical strategy using a fusion image constructed from ^{11}C-methionine PET, ^{18}F-FDG-PET and MRI for glioma with no or minimum contrast enhancement. *J Neurooncol* 138: 537–548, 2018
15) Kim DS, Na DG, Kim KH, et al.: Distinguishing tumefactive demyelinating lesions from glioma or central nervous system lymphoma: added value of unenhanced CT compared with conventional contrast-enhanced MR imaging. *Radiology* 251: 467–475, 2009
16) Lebrun C, Bensa C, Debouverie M, et al.: Association between clinical conversion to multiple sclerosis in radiologically isolated syndrome and magnetic resonance imaging, cerebrospinal fluid, and visual evoked potential: follow-up of 70 patients. *Arch Neurol* 66: 841–846, 2009
17) Singhal T, Narayanan TK, Jain V, Mukherjee J, Mantil J: ^{11}C-L-methionine positron emission tomography in the clinical management of cerebral gliomas. *Mol Imaging Biol* 10: 1–18, 2008
18) Takenaka S, Shinoda J, Asano Y, et al.: Metabolic assessment of monofocal acute inflammatory demyelination using MR spectroscopy and (11)C-methionine-, (11)C-choline-, and (18)F-fluorodeoxyglucose-PET. *Brain Tumor Pathol* 28: 229–238, 2011
19) Padma MV, Adineh M, Pugar K, et al.: Functional imaging of a large demyelinating lesion. *J Clin Neurosci* 12: 176–178, 2005
20) Yasuda S, Yano H, Kimura A, et al.: Frontal tumefactive demyelinating lesion mimicking glioblastoma differentiated by methionine positron emission tomography. *World Neurosurg* 119: 244–248, 2018
21) Albert NL, Weller M, Suchorska B, et al.: Response Assessment in Neuro-Oncology working group and European Association for Neuro-Oncology recommendations for the clinical use of PET imaging in gliomas. *Neuro-oncology* 18: 1199–1208, 2016
22) Tsuyuguchi N, Sunada I, Ohata K, et al.: Evaluation of treatment effects in brain abscess with positron emission tomography: comparison of fluorine-18-fluorodeoxyglucose and carbon-11-methionine. *Ann Nucl Med* 17: 47–51, 2003
23) Nakajima R, Kimura K, Abe K, Sakai S: ^{11}C-methionine PET/CT findings in benign brain disease. *Jpn J Radiol* 35: 279–288, 2017
24) Ishii K, Ogawa T, Hatazawa J, et al.: High L-methyl-[11C]methionine uptake in brain abscess: a PET study. *J Comput Assist Tomogr* 17: 660–661, 1993
25) Hirata K, Shiga T, Fujima N, et al.: (11)C-Methionine positron emission tomography may monitor the activity of encephalitis. *Acta Radiol* 53: 1155–1157, 2012

Address reprint requests to: Motoki Inaji, MD, PhD, Department of Neurosurgery, Tokyo Medical and Dental University, 1-5-45 Yushima, Bukyo-ku, Tokyo, Japan. *e-mail*: inamnsrg@tmd.ac.jp